Spin Torque Nano-Oscillators as candidates for Artificial Neural Networks

Author: Sergi Cruz Desentre.
Facultat de Física, Universitat de Barcelona, Diagonal 645, 08028 Barcelona, Spain.

Abstract: Artificial Neural Networks have been widely used with great success for tasks such as input classification. However, they require considerable computing resources. Spin Torque Nano-Oscillators are nanometric devices capable of converting an spin-polarized current into a magnetic oscillation, through the spin-transfer-torque effect. We show that this devices are capable of non-linear behavior such as synchronization, and that their oscillation can be finely adjusted, making them good candidates for efficient, hardware-built neural networks.

I. INTRODUCTION

Artificial **N**eural **N**etworks are brain-inspired computing systems, composed of interacting artificial neurons organized in layers as seen in Fig. 1. Each neuron computes a non-linear function of its inputs, and sends its output to other neurons through weighted connections. The result is given by the neurons at the output layer.

ANN are capable of "learning" by finely adjusting the weight of their neuron connections. This is done by exposing the ANN to inputs with a known desired output, and tuning the weights so as to minimize errors. However, ANN require considerable energy and computing resources [1]. While a brain has "hardware-built" neurons, the computing artificial neurons must be simulated, as does each individual connection. Nevertheless, recent works have shown that oscillators capable of synchronization are good candidates for hardware neurons.[2][3]

Spin **T**orque **N**ano-**O**scillators are nanometric devices comprised of a fixed and a free ferromagnetic film divided by a layer of non-magnetic metal, as seen schematically in Fig, 2. A spin-polarized electrical current applied to the STNO excites the magnetic moment of the free layer, and causes an oscillation of the magnetization with a frequency highly dependent on the applied current's intensity. In addition, this oscillation is extremely sensitive to periodic electric or magnetic signals, including other STNO, and is the cause of synchronization.

We will show that non-linear behavior and high tunability make STNOs ideal candidates for compact and efficient hardware neural networks.

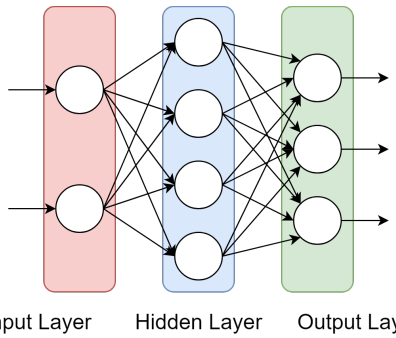

FIG. 1: Schematic of a neural network. The neurons (circles) are organized in layers (rectangles), and interact with each other following the arrows.

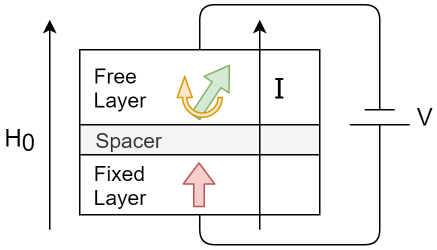

FIG. 2: Schematic of a Spin Torque Nano-Oscillator. The free and fixed layers are ferromagnetic, while the spacer is a non-magnetic metal layer. The electrical current applied induces the precession of the free layer's magnetic moment around the direction of the external field $H_0\mathbf{z}$.

II. MATHEMATICAL MODELLING

In order to describe the current-induced oscillations of the STNO's magnetic moment, we use the Landau-Lifshitz-Gilbert-Slonczewski equation [4], considering the STNO a thin ferromagnetic film. This gives us

$$\begin{aligned}\frac{\partial \mathbf{M}}{\partial t} =& -|\gamma|\,\mu_0 \mathbf{M}\times\mathbf{H}_{\text{eff}} \\ &- \alpha\frac{|\gamma|\,\mu_0}{M_s}\mathbf{M}\times(\mathbf{M}\times\mathbf{H}_{\text{eff}}) \\ &+ \beta(\mathbf{M}\times\mathbf{M}\times\mathbf{m}_p),\end{aligned} \tag{1}$$

where M is the magnetization vector, γ is the electron's gyromagnetic ratio, μ_0 is the permeability of free space, M_s is the saturation magnetization and $\mathbf{m}_p$ is the direction of the applied current's spin polarization. $\mathbf{H}_{\text{eff}}$ is the effective magnetic field taken as $\frac{\partial \mathbf{E}}{\partial \mathbf{M}}$.

In our case, as our sample is a thin magnetic film and the field is applied perpendicular to the film's plane, $\mathbf{H}_{\text{eff}}$ is taken as the sum of the external field H_0 and the demagnetizing field

$$\mathbf{H}_{\text{eff}} = (H_0 - M_z)\mathbf{z}. \tag{2}$$

In practice, the effective field $\mathbf{H}_{\text{eff}}$ in Eq. 2 should also include the exchange field, proportional to $\nabla^2\mathbf{M}$. However, due to the very small size of an STNO, the oscillations of $\mathbf{M}$ can be considered spatially uniform and this term

vanishes.

Eq. (1) has three terms. The first one induces a precession of the magnetization around the external field. The second one, controlled by the dimensionless damping constant α, tries to slow down this precession until the magnetization and the external field are aligned. The third one is the spin-transfer torque term, which induces a reverse damping around the direction of the applied current's polarization $\mathbf{m}_p$. It is controlled by the parameter β, which is linearly dependent on the intensity of the applied current. The effect of this three terms on the magnetization can be seen schematically on FIG. 3.

The parameter β also depends on the STNO's geometry and its material properties, such as the film's thickness, the radius of its contact points and its spin-torque efficiency. Nevertheless, this parameter can be considered as $\beta = \beta_0 I$, where β_0 is a constant and I is the applied current's intensity.

If we define the following dimensionless parameters

$$\mathbf{m} = \frac{\mathbf{M}}{M_s} = (m_x, m_y, m_z)$$

$$\tau = \gamma \mu_0 M_s t \qquad\qquad h = \frac{H_0}{M_s},$$

we can use them to normalize Eq. (1) and rewrite it as

$$\begin{aligned} \frac{\partial \mathbf{m}}{\partial \tau} =& -\mathbf{m} \times \mathbf{h}_{\text{eff}} - \alpha \mathbf{m} \times (\mathbf{m} \times \mathbf{h}_{\text{eff}}) \\ &+ \beta(\mathbf{m} \times \mathbf{m} \times \mathbf{m}_p), \end{aligned} \tag{3}$$

where $\mathbf{h}_{\text{eff}}$ is

$$\mathbf{h}_{\text{eff}} = (h - m_z)\mathbf{z}. \tag{4}$$

For a typical STNO with a permalloy film as the free layer, α is roughly of order 10^{-2}. A value of $\alpha = 0.01$ is the one considered throughout our analysis. If the applied current has enough intensity and its spin polarization $\mathbf{m}_p$ is aligned with the effective field $\mathbf{h}_{\text{eff}}$, the spin torque term can overcome the damping and induce an oscillation of the magnetization at a wide range of frequencies, depending on parameter β and the external field h.

The frequency of this oscillation can then be finely tuned by changing the intensity of the applied current (and thus changing β). We will show this in the following section.

III. SIMULATION AND ANALYSIS

We will first simulate the time-evolution of a single STNO's magnetization under a constant external magnetic field applied perpendicular to the film's plane. Equation 3 was solved by the lsoda FORTRAN function through Python's scipy library.

In absence of β, the system should evolve until its magnetization points towards the external field's direction.

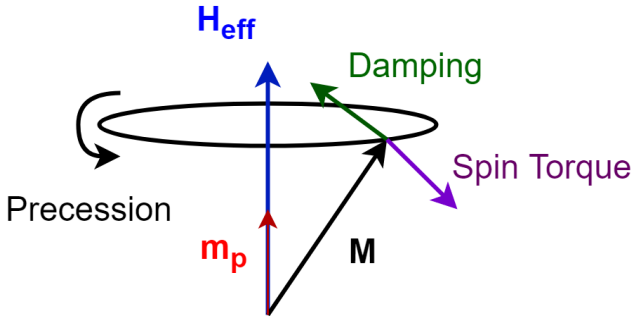

FIG. 3: Diagram showing the contribution of each of the Landau-Lifshitz-Gilbert-Slonczewski equation's terms. The first one induces a precession of the magnetization $\mathbf{M}$ around the effective field $\mathbf{H}_{\text{eff}}$. The damping term aligns the magnetization with the effective field, decreasing the amplitude of the oscillation, while the spin torque term is equivalent to a reverse damping in the direction of the applied current's spin polarization $\mathbf{m}_p$.

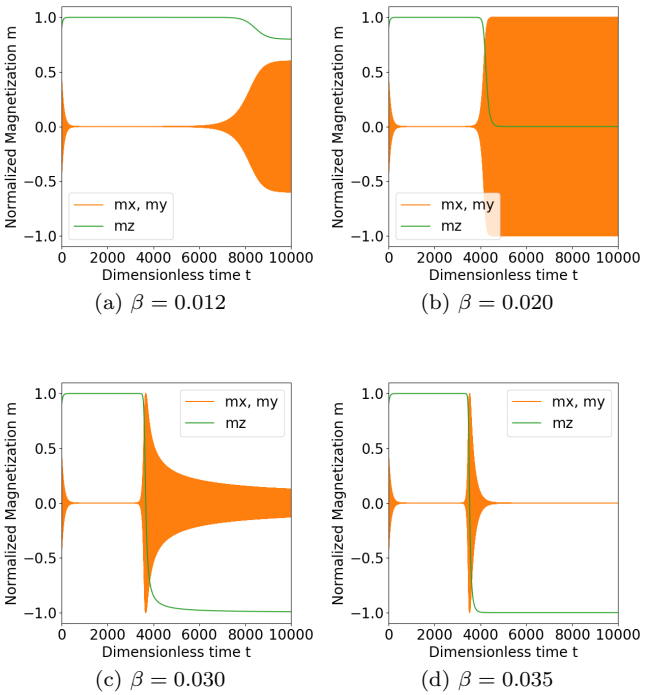

(a) $\beta = 0.012$ (b) $\beta = 0.020$

(c) $\beta = 0.030$ (d) $\beta = 0.035$

FIG. 4: Time-evolution of the magnetization under different values of β. The STNO first settles in the direction of the external field h, as no current is applied ($\beta = 0$). At time $\tau = 3000$, β is set to the labelled value and the magnetization oscillates in the x-y plane at a certain height m_z, as schematically seen in Fig. 3. No oscillation is observed at $\beta < 0.009$ (damping is stronger than spin torque), or at $\beta > 0.034$ (magnetization is completely reversed).

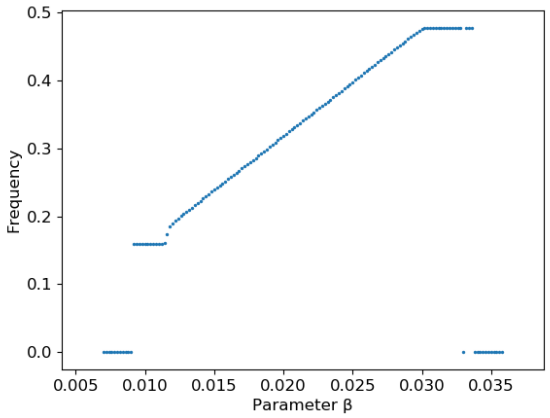

FIG. 5: Frequency (as the inverse of dimensionless time τ) of the magnetization's oscillation as a function of β, for an STNO with damping constant $\alpha = 0.01$ under constant external magnetic field $h = 2$.

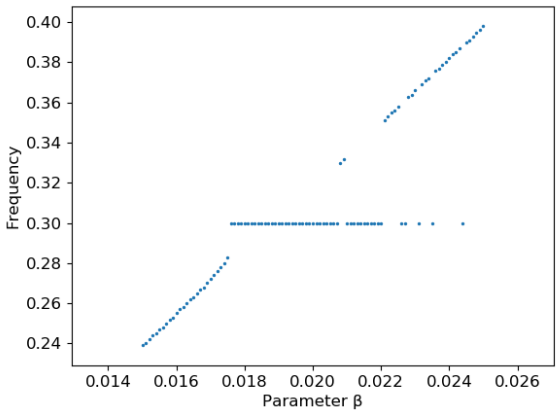

FIG. 6: Frequency of the magnetization's oscillation as a function of β, for an STNO under an oscillating magnetic field with $\epsilon = 0.02$ and $\omega = 0.3\tau^{-1}$, where synchronization of the STNO can be observed.

Since we are applying the magnetic field in the **z** direction, perpendicular to the film's plane, we will need to overcome the STNO's demagnetizing field. To achieve this, h should be greater than 1, that is, the external field H_0 should overcome the saturation magnetization M_s. For this reason, the dimensionless external field is set to $h = 2$.

The time-evolution of m_x, m_y and m_z is shown in Fig. 4, as a function of τ and under different values of β. The system starts at $\tau = 0$ in a non-equilibrium state, but the magnetization quickly settles in the external field's direction **z**, where $m_z = 1$. At $\tau = 3000$, electrical current is applied to the STNO (β goes from zero to its labelled value). This causes m_z to settle at a lower height, while m_x and m_y oscillate in the x-y plane.

No oscillation can be observed for values under $\beta = 0.009$, since it is over this threshold where the spin-torque term at Eq. 3 overcomes the damping, and corresponds to the intensity of the critical current. As β increases, m_x and m_y keep oscillating while m_z approaches -1. At values over $\beta = 0.034$, $m_z = -1$, and oscillation in the x-y plane becomes impossible.

By taking the Fourier Transform of the magnetization's oscillation in the x-y plane, we can find its frequency. By measuring it over a range of values of β, we can see in Fig. 5 that the frequency increases linearly with β.

A. Synchronization with an external frequency

Due to the high sensitivity of their oscillation frequency on the amplitude of the oscillation, STNOs are capable of synchronization with other frequencies through electric currents or magnetic fields. When synchronization happens, the STNO's frequency becomes the same as the external one, with a fixed phase between the two. In order to observe this property, we can modify Eq. 4 to include an oscillating component

$$\mathbf{h}_{\text{eff}} = (h - m_z)\mathbf{z} + \epsilon \sin(\omega\tau)\mathbf{x}, \tag{5}$$

where ω is the frequency and ϵ the amplitude of the effective magnetic field's oscillating component. Note that, as the STNO oscillates in the x-y plane, the same must be true for the magnetic field so as to achieve synchronization.

Synchronization between an STNO and the oscillating component of the magnetic field can be seen on FIG. 6, where the STNO's frequency is plotted as a function of β, and the amplitude ϵ of the oscillating component is small compared to the magnetic field ($\epsilon = 1\%$ of h). Increasing ϵ results in a widening of the locking range, that is, the range of external frequencies where the STNO's precession frequency will get pulled towards synchronization.

B. Multiple interacting STNOs

When additional STNOs are included in the system, they influence each other through the oscillating magnetic field generated by their precessing magnetic moment **m**. This can be modelled by adding an extra component to the effective field felt by each STNO, changing Eq. 5 to

$$\mathbf{h}_{\text{eff}_i} = (h - m_{z_i})\mathbf{z} + \epsilon \sin(\omega\tau)\mathbf{x} + \sum_{i \neq j}^{N} \varepsilon_{i,j}\mathbf{m}_j \tag{6}$$

where $\mathbf{h}_{\text{eff}_i}$ is the effective magnetic field felt by the ith STNO, N is the number of STNOs in the system and $\varepsilon_{i,j}$ is the coupling constant between the ith and jth STNO. We now have to compute the time-evolution of

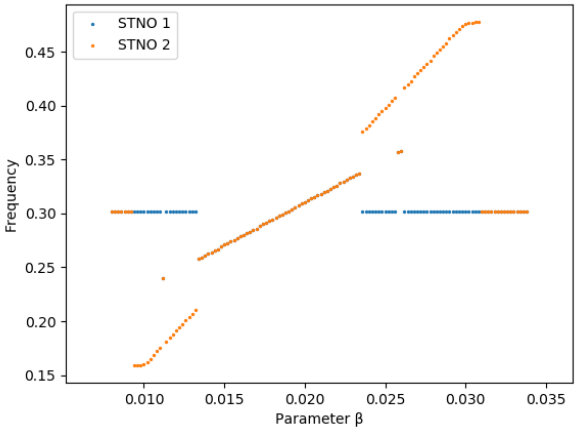

FIG. 7: Oscillation frequency of two STNOs as a function of the second one's β, with the first one's β fixed at a constant value of $\beta = 0.020$ under a constant field $h = 2$. The coupling constant has a value of $\varepsilon_{1,2} = 4 * 10^{-3}$, equivalent to a 0.2% of h.

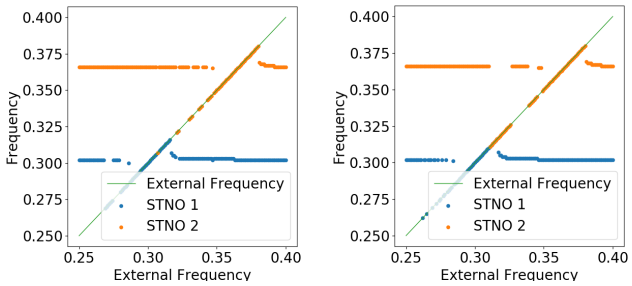

(a) $\varepsilon_{1,2} = 0$ (b) $\varepsilon_{1,2} = 2.5 * 10^{-3}$

FIG. 8: Oscillation frequency of two STNOs as a function of the external field's frequency. In both (a) and (b) the STNOs β is fixed to values $\beta_1 = 0.019$ and $\beta_2 = 0.023$ respectively, with the only difference between (a) and (b) being the labelled value of the coupling constant $\varepsilon_{1,2}$ between STNOs. This causes in (b) the synchronization of STNO 2 with the external frequency and STNO 1 around frequencies of $0.31\tau^{-1}$.

each STNO's magnetization $\mathbf{m}_i$ as a system of N coupled differential equations, due to $\mathbf{m}_i$ depending on $\mathbf{h}_{\text{eff}i}$, and thus depending on all the other STNO's magnetization $\mathbf{m}$.

The coupling constant ε depends mainly on the distance and spatial disposition of the oscillators, and represents how much they "feel" each other. However, synchronization can be easily achieved for very low values of ε, on the order of $\varepsilon_{i,j} \sim 10^{-3}$. This is shown on Fig. 7, where synchronization is observed with $\varepsilon = 4 * 10^{-3}$ between two STNOs under a constant external field h.

Multiple STNOs can be set at different frequencies, adjusting the intensity of the electrical current applied to each one. Then, when the external field oscillates at a given frequency, we can detect which (if any) of the oscillators have synchronized to it.

We can consider the external frequency ω as the input of our system, and the synchronization state of each of the STNOs ("synchronized" or "unsynchronized" to the input frequency) as the output. The combination of all possible states for the N STNOs become the synchronization configurations, which can be identified as "bins" where our given input can fall into. The size and location of these bins can be finely tuned by adjusting the intensity of the current (and thus β) applied to each STNO.

The emergent property of synchronization between STNOs adds a non-linear behavior to the system, further increasing the complexity of the output bins' shape that it is able to generate. This can be seen in Fig. 8, where the frequency of two STNOs is shown as a function of the external field's frequency. In Fig. 8 (a) there is no interaction between them, while in Fig. 8 (b) the interaction between oscillators creates an additional configuration where both STNOs have coupled with the external frequency around $f = 0.31\tau^{-1}$.

C. Synchronization with multiple frequencies

We are not limited to just one input. An arbitrary number M of external frequencies can be added to the effective magnetic field $\mathbf{h}_{\text{eff}i}$ felt by each STNO:

$$\mathbf{h}_{\text{eff}i} = (h - m_{zi})\mathbf{z} + \sum_{k=1}^{M} \epsilon_k \sin(\omega_k \tau)\mathbf{x} + \sum_{i \neq j}^{N} \varepsilon_{i,j}\mathbf{m}_j \quad (7)$$

where ω_k is the kth frequency and ϵ_k is the effective field's amplitude of the kth oscillating component.

Multiple input frequencies greatly increase the number of possible synchronization states, as now a given STNO can be phase-locked to any (or none) of the input frequencies, when before its only possible states where "synchronized" or "unsynchronized".

A relatively simple example can be seen in Fig. 9, where we show the synchronization configurations of two oscillators as a function of two input frequencies. By adjusting only one of the STNO's applied current from (a) ($\beta_1 = 0.018$) to (b) ($\beta_1 = 0.020$), we can see the change in shape and location of the synchronization configurations that divide the input space.

For example, the "1B2A" and "1A2B" configurations (where STNO 1 is synchronized with frequency B and STNO 2 is synchronized with frequency A, and vice versa) have a simple, almost square shape in (a). However, in (b), these regions have moved and their shape has changed, now having a separate diagonal "strand" surrounded by the "2A" and "2B" regions. Also, the configurations "1A2A" and "1B2B", while almost non-existent in (a), have formed in (b) vertical and horizontal "stripes" respectively, sprinkled between "1A" and "2A", and "1B" and "2B".

The high symmetry of Fig. 9 around the diagonal is to be expected, as both frequency A and B have the same

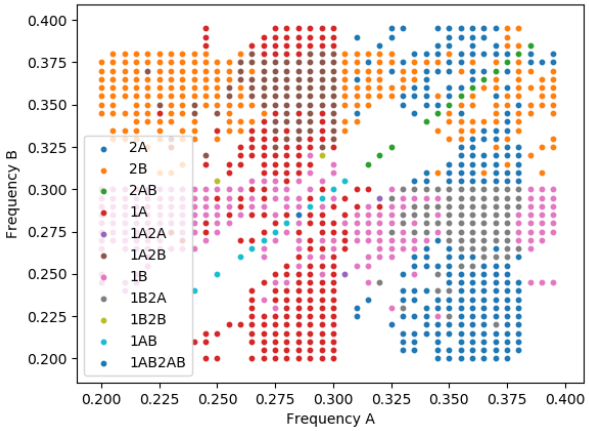

(a)
$\beta_1 = 0.018$ ($f_1 = 0.286\tau^{-1}$)
$\beta_2 = 0.023$ ($f_2 = 0.366\tau^{-1}$)

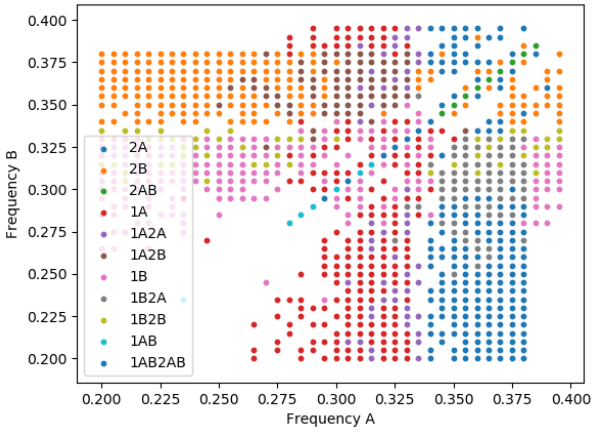

(b)
$\beta_1 = 0.020$ ($f_1 = 0.318\tau^{-1}$)
$\beta_2 = 0.023$ ($f_2 = 0.366\tau^{-1}$)

FIG. 9: Synchronization configurations of two STNOs as a function of two input frequencies A and B. The configurations are labeled with an STNO's index and the letter(s) of the synchronized frequencies. For example, "1A2B" means "oscillator 1 synchronized with frequency A, oscillator 2 synchronized with frequency B".

amplitude ϵ as components of the effective magnetic field $\mathbf{h}_{\text{eff}}$. In such conditions, the point ($f_A = 0.2$, $f_B = 0.3$) in input space is equivalent to ($f_A = 0.3$, $f_B = 0.2$).

We can now identify all the characteristic elements present in a typical neural network as shown on Fig. 1. The neurons at the input layer are equivalent to the frequencies of the external field's oscillating components. The neurons at the hidden layer, the STNOs, interact with the input layer and with each other through synchronization. These interactions can be adjusted, changing the intensity (and thus β) of an STNO's applied current, and modifying the spatial disposition (and thus the coupling constant ε) of the STNOs. Finally, the neurons at the output layer correspond to the synchronization configurations, and classify the input into one of multiple bins.

IV. CONCLUSIONS

We have successfully simulated multiple Spin Torque Nano-Oscillators, and shown the high tunability of their oscillation's frequency and their ability to synchronize with external frequencies and other STNOs. These are needed behaviors for artificial neurons: both the non-linearity of their output and the fine-tuning of their connections.

We have also established a link between our simulated system and the constituent elements of an artificial neural network. The external frequencies being the input neurons, the STNOs being the neurons at the hidden layer, their frequency and coupling constant being the adjustable weighted interactions, and the synchronization configurations being the output.

However, it remains to be seen whether an STNO hardware neural network could be assembled in practice, learn from training data, and produce results with similar accuracy as a computer artificial neural network. Nevertheless, all the pieces are there for future work on this promising subject.

Acknowledgments

I would like to extend my gratitude to my advisor, Ferran Macià, for his guidance and encouragement. To my parents, for their financial and emotional support, and to my brother, my close friends and my colleagues. Neither me nor this work could have been the same without you.

[1] Chris Edwards. Growing pains for deep learning. *Commun. ACM* **58**, 7, 14–16 (2015).
[2] Fang, Y., Yashin, V. V., Levitan, S. P. & Balazs, A. C. Pattern recognition with "materials that compute". *Sci. Adv.* **2**, e1601114 (2016).
[3] Macià, F., Kent, A. D. & Hoppensteadt, F. C. Spin-wave interference patterns created by spin-torque nano-oscillators for memory and computation. *Nanotechnology* **22**, 095301 (2011).
[4] Slonczewski J C Current-driven excitation of magnetic multilayers *J. Magn. Magn. Mater.* **159** L1–7 (1996).